15085 PORPHYRITIC SUBOPHITIC QUARTZ-NORMATIVE MARE BASALT ST. 1 471.3 g

INTRODUCTION: 15085 is a coarse-grained basalt (Fig. 1), with large, zoned pigeonite crystals. It has been dated as close to 3.40 b.y. old. The sample is blocky and subrounded. It is generally tough or coherent, but there are penetrative fractures which make some portions quite friable. It is light brownish gray overall, but consists of yellow-brown mafic minerals and white plagioclases. It has no zap pits but about 2% vugs into which pyroxene and plagioclase grains project.

15085 was collected on the east flank of Elbow Crater, as one of five basalt samples collected on a line extending out from the crater (see Fig. 15065-1). It was collected with breccia 15086 about 60 m from the rim crest, in a flat area with distinctly spaced cobbles such as 15085. Its orientation is known.

PETROLOGY: 15085 is a coarse, quartz-normative mare basalt, lacking magnesian olivine but containing zoned pigeonite crystals (Fig. 2). These are less-easily described as phenocrysts in 15085 than in other quartz-normative basalts because the plagioclases are also very large (both pigeonite and plagioclase up to about 1 cm), although the plagioclase is less abundant and most is smaller. The pigeonites have simple twins, and zone to augite; in many cases the pigeonite to augite transition is very sharp. The rims contain inclusions; discrete augite grains also occur in the groundmass. The plagioclases are slightly zoned optically. Tridymite blades are a common accessory, frequently embedded in pyroxferroite, and there are small patches of mesostasis consisting of tridymite laths, glass, and opaque phases, cristobalite occurs as irregular patches. Opaque phases range from chromite (in pigeonite cores) to ulvospinel and residual ilmenite. Some patches consist of brown material consisting of a fine-grained intergrowth of (probably) silica, fayalite, and a second mafic phase; these patches pseudomorph pyroxferroite(?) and some pyroferroite grains contain patches of this assemblage.

The Lunar Sample Information Catalog Apollo 15 (1972) reported a mode of 66% clinopyroxene, 22% plagioclase, 4% tridymite, 2% pyroxferroite, 1.5% ilmenite, 1.5% ulvospinel, and less than 0.1% each of Fe-Ni metal, troilite, Cr-spinel, and an unidentified phase. Mason (1972) reported that the sample contained 0.7% (wt) tridymite and 0.4% (wt) cristobalite. Papanastassiou and Wasserburg (1973) noted that plagioclase was fractured and there was clear indication of shock, but shock features are not apparent in most of the sample.

The pyroxenes are extensively zoned (Brown et al., 1972a,b), but the low-Ca pigeonite cores are extensive (60% or so of each crystal) (Fig. 3). The zoning is mainly to subcalcic ferroaugite; augite itself is rare. Some cores are subcalcic pigeonites (2.2% CaO) and might be hypersthene (Brown et al. (1972b). Rims have Ti/Al less than 1/2,

suggesting that Ti^{3+} is present. Takeda et al. (1975) made single crystal x-ray diffraction studies of pyroxenes, tabulating cell dimensions, relative orientations, and space groups ($P2_1/c$ for pigeonite, C2/c for augite). Microprobe analyses showed zoning from $En_{67.5}Wo_{5.1}$ to $En_{42.6}Wo_{36.7}$. The pigeonites have augite oriented on both (001) and (100) but a lack of distinct core/rim relations in the sample studied make it difficult to distinguish epitaxial growth from an exsolution relationship. Exsolution is not visible optically. A subcalcic augite exsolved pigeonite on (001), with $\Delta\beta$ for the pair being 2.4°.

Figure 1. Pre-split view of 15085. S-71-45889

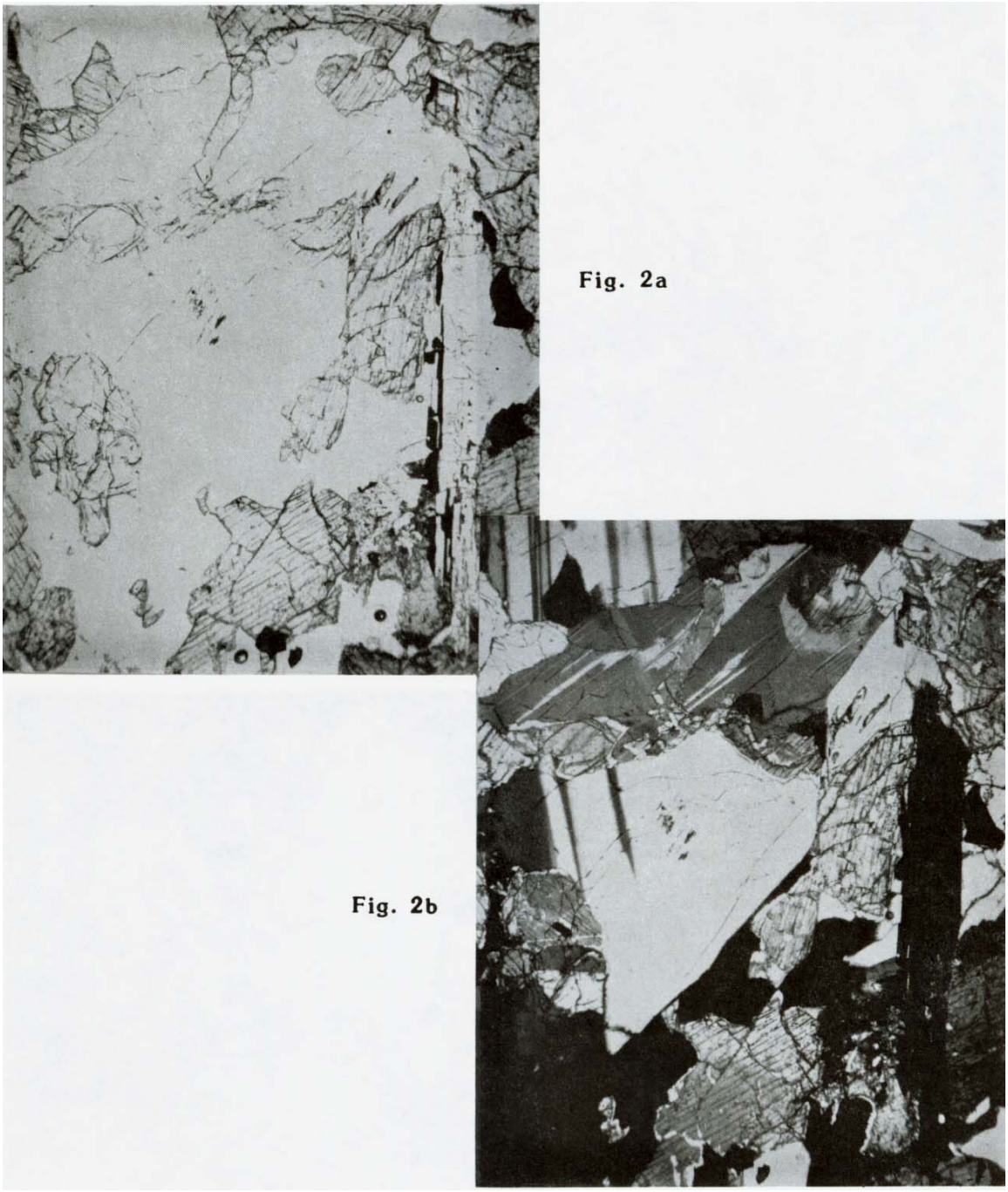

Figure 2. Photomicrographs of 15085,11. Widths about 3 mm.
a)c) transmitted light, b)d) crossed polarizers,
a)b) coarse groundmass with large plagioclases. Lath at right is tridymite,
c)d) two zoned pigeonites (lower is twinned, and part of a 1 cm grain).
Middle right are tridymite laths intergrown with opaque phases.
Upper right are tridymite laths embedded in a 1 mm grain of pyroxferroite.

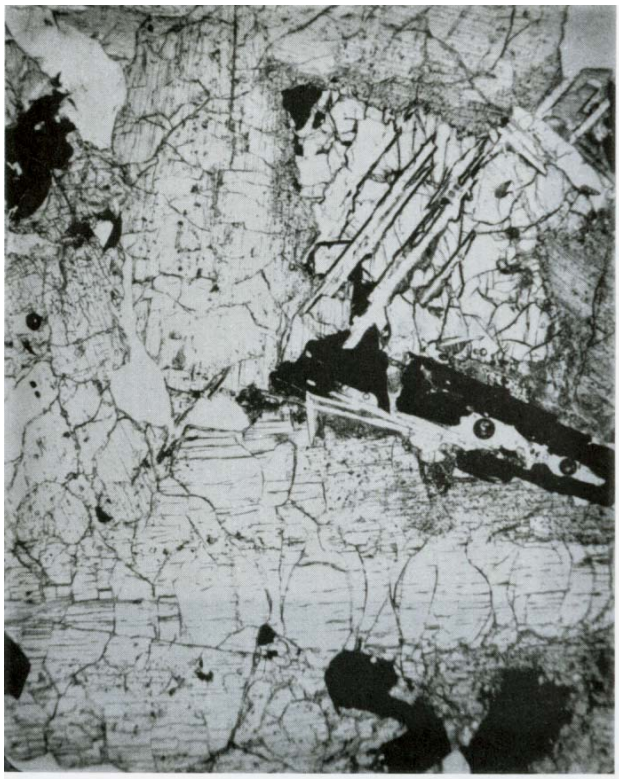

Fig. 2c

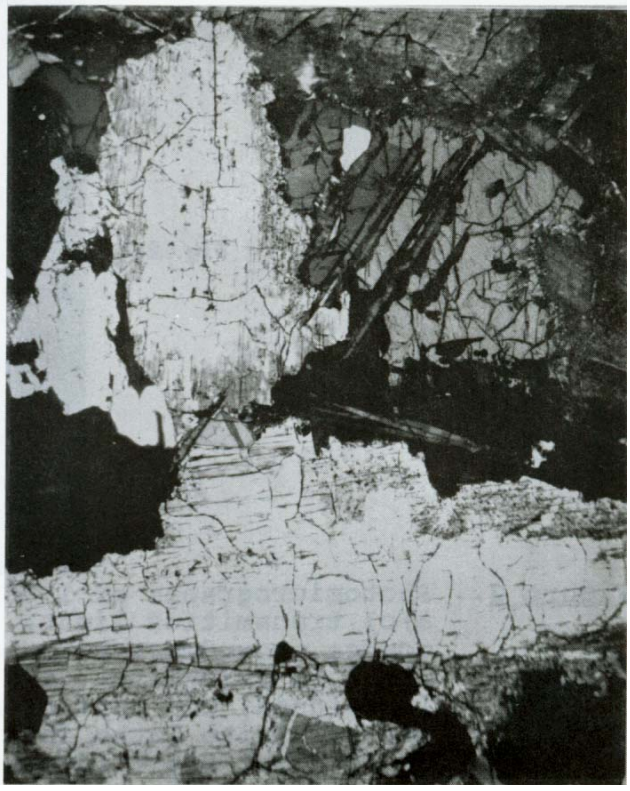

Fig. 2d

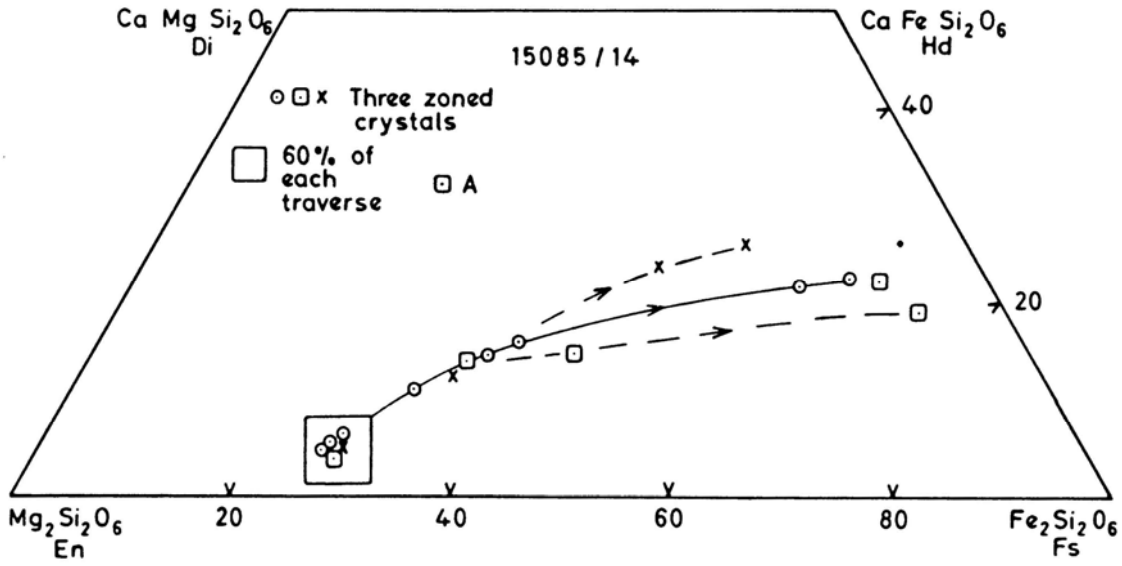

Figure 3. Pyroxene compositions (Brown et al., 1972b)

Mason (1972) described and analyzed the tridymite and cristobalite crystals. The tridymite occurs as thin platy crystals (narrow laths in section) (see Fig. 2) and the cristobalite as anhedral grains showing a mosaic texture attributed to inversion. Tridymite also shows patchy extinction attributable to inversion. Both have low birefringence: tridymite about 0.003, cristobalite about 0.001. The analyses (Table l) show them to be more than 99% SiO_2, but with appreciable TiO_2. The molecular ratio of Al_2O_3 to ($Na_2O + K_2O + CaO$) is close to unity, suggesting replacement is of the type K + Al<=>Si. There appears to be little chemical difference between the two polymorphs, except perhaps lower K_2O and Al_2O_3 in the cristobalite. The tridymite indicates that crystallization was completed at 1000°C or less; the cristobalite clearly crystallized outside its thermodynamic stability field.

L. Taylor et al. (1975) reported analyses of spinel phases, ranging from Ti-chromites to Cr-ulvospinel (Fig. 4). They do not display the "core-rim" textures common in Apollo 12 spinels. Brown et al. (1972b) and Papanastassiou and Wasserburg (1973) each listed an analysis of a spinel. L. Taylor et al. (1975) also reported Fe-metal analysis (Fig. 5). The metals include some with unusually high Ni compared with other mare basalts, up to 58.2 wt%.

Cooling Rates: Lofgren et al. (1975), in a comparison of the natural rock textures with those produced in dynamic crystallization experiments, deduced cooling rates of <1°C/hr for both the pigeonites and for the groundmass, and 15085 appeared to have cooled the slowest among those studied. Grove and Walker (1977) determined a late-stage cooling rate of 0.01°C/hr from the plagioclase dimensions, also as compared with the products of dynamic crystallization experiments. The sample seems to have experienced a slow, nearly linear cooling rate throughout its entire cooling history. L. Taylor et al. (1975) used the partitioning of Zr between ilmenite and ulvospinel to determine a cooling rate of

7°C/day, in agreement with the Lofgren et al. (1975) estimate of less than 24°C/day. The underlying model was improved by Onorata et al. (1979) with experimental determination of the diffusion of Zr, revising the cooling rate to 1.00 to 2.8°C/day. A model taking grain size into account was also investigated. Takeda et al. (1975), on the basis of Δβ (2.4°) for an augite-pigeonite exsolution pair, suggested that 15085 was slowly cooled, but not as slowly as 15058 or 15475 (a minor reversal of the sequence as determined from experimentally determined textures).

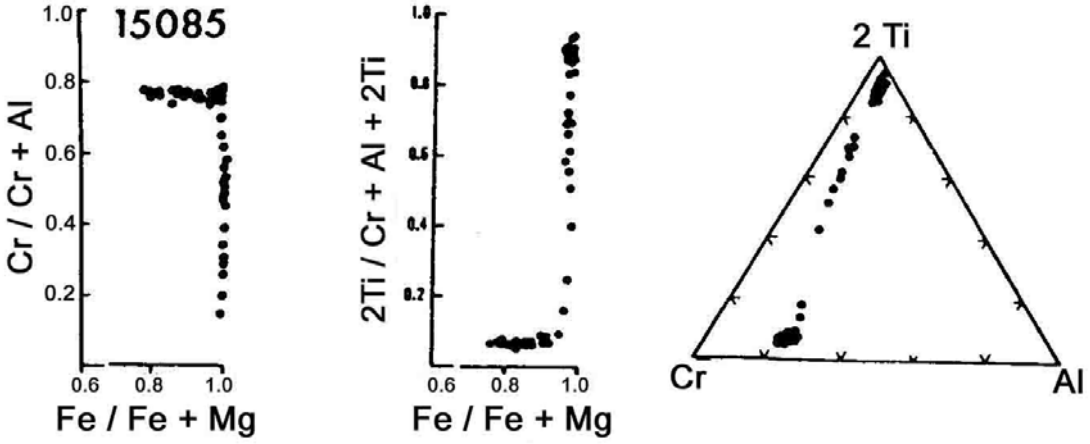

Figure 4. Spinel compositions
(Taylor et al., 1975).

TABLE 15085-1. Analyses of tridymite and cristobalite
(Mason, 1972)

	tr	cr
SiO2	[99.05]	[99.13]
TiO2	.28	.38
Al2O3	.34	.18
FeO	<0.02	.09
MnO	<0.02	<0.02
MgO	<0.03	<0.03
CaO	0.02	<0.02
Na2O	0.05	0.05
K2O	0.26	0.17
P2O5	<0.03	<0.03

CHEMISTRY: Bulk rock analyses are listed in Table 2, with rare earths shown in Figure 6. There are some severe discrepancies among samples which are a result of the small sample sizes and the coarse grain size. The analysis of Rhodes and Blanchard (1983 and unpublished) is based on the most representative sampling: 10 g were reduced to medium sand size and then 2 g were used for the analysis. This analysis (data not available) removes any doubt that 15085 is a member of the quartz-normative basalt group.

Sampling problems and discrepancies among splits had been referred to by previous workers (e.g., Mason et al., 1972). Ganapathy et al. (1973) found the siderophiles and volatiles to be similar to those in fine-grained sample 15597, indicating that there was little fractionation of these elements during shallow-level crystallization. Helmke and Haskin (1972) put 15085 in a group of high Sm/Eu quartz-normative basalts.

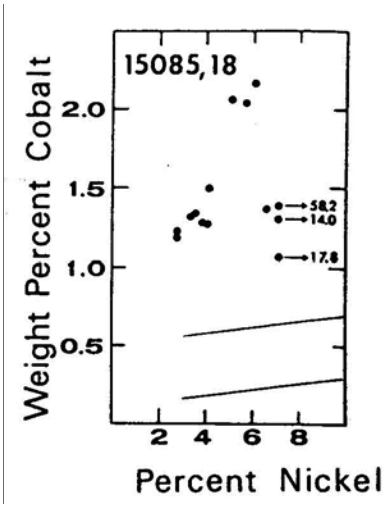

Figure 5. Metal compositions (Taylor et al., 1975).

Gibson et al. (1975) reported data for C in CO (3.3 ppm C); in CO_2 (7.8 ppm C); for H in H_2 (9.7 ppm); and for S in H_2S (559 ppm S; acid hydrolysis). They also reported abundances of Fe^0 of 542 and 340 ppm from hydrolysis and magnetic techniques respectively. Wanke et al. (1976) also reported a determination for oxygen.

Helmke et al. (1972) and Helmke and Haskin (1973) tabulated trace element data for separated minerals, in a study of the effects of closed-system crystallization (Fig. 7). The patterns are not distribution coefficients, although that for pigeonite could be close to one. The unusual pattern for augite can be understood in terms of closed-system crystallization. Jovanovic and Reed (1977) reported mineral separate data for Hg, Ru, and Os, and for the Hg released from these minerals at less than 130°C. The Ru and Os in the minerals (combined) were 6x as much as these in the whole rock, but the Ru/Os ratio was the same; apparently these elements are not uniformly distributed in the rock.

STABLE ISOTOPES: Gibson et al. (1975) reported $\delta^{34}S_{CDT}$ °/oo of -1.3, of the sulfur produced during their total combustion. This isotopic ratio is similar to that of other mare basalts.

RADIOGENIC ISOTOPES AND GEOCHRONOLOGY: Papanastassiou and Wasserburg (1973) reported a Rb-Sr two point isochron age of 3.40 ± 0.04 b.y. with an initial $^{87}Sr/^{86}Sr$ ratio of 0.69923 ± 6 b.y. The tabulated data are for the separates plagioclase and "ilmenite".

Tatsumoto et al. (1972) reported U, Th, and Pb isotopic data for a whole rock sample, which falls on a 3.5 to 4.65 b.y. discordia line ($^{206}Pb/^{238}U$ vs. $^{207}Pb/^{235}U$) when plotted with 15065, 15076, and 15476. Unruh and Tatsumoto made a detailed study of the U, Th, and Pb isotopic systems for whole rock and mineral separate samples of 15085. They tabulated data for separates, including leaches (HCl) and residues. Significant portions

TABLE 15085-2. Bulk rock chemical analyses

		,21	,34	,6	,8	,71	,0	,5	,34	,39	,97	,47	,47	,50	,71(b)	,71(b)
	SiO2		46.39						46.61	47.73				48.06		
	TiO2		3.07	1.67	2.60				2.63	1.96				1.57		
	Al2O3		5.79	10.0	6.61				7.13	9.92				11.17		
	FeO		26.75	18.3	23.0				24.38	19.69				18.42		
	MgO		8.20						7.90	8.84				7.85		
	CaO		9.12						9.68	10.63				11.23		
	Na2O		0.21	0.309	0.243				0.26	0.33				0.365		
	K2O		0.07				0.048		0.059	0.035				0.54		
	P2O5		0.09						0.107	0.064		0.068		0.055		
(ppm)	Sc			41	51									44.0		
	V		110						172	165						
	Cr		4600	3350	3980				4200	3570				2940		
	Mn	2420	2870						2300	2160				2010		
	Co		49	42	48				43	41				35.7		
	Ni	37	45						20	23				31		
	Rb		<5					0.86	1.8	<1.5				0.73		
	Sr		92						120	112				107		
	Y		54						44.0	28.6				21		
	Zr		150						156	92				99		
	Nb								10.0	6.6						
	Hf			2.0	3.1									2.44		
	Ba	68	87						110	60				62.1		
	Th					0.4588	0.57							0.42	0.405	0.426
	U					0.1183	0.138	0.135				0.16		0.13	0.106	0.111
	Pb		2			0.208									0.186	0.174
	La	4.92		4.5	6.5									5.88		
	Ce	13.2												16.5		
	Pr													2.5		
	Nd	10.2												13.1		
	Sm	3.86		3.15	4.5									3.79		
	Eu	0.84		1.02	1.12									1.07		
	Gd	4.9												5.4		
	Tb	0.90		0.7	1.1									0.92		
	Dy	5.79												5.65		
	Ho	1.16												1.2		
	Er													3.5		
	Tm															
	Yb	2.63		2.0	3.1									2.72		
	Lu	0.393		0.36	0.53									0.43		
	Li		8									6.5		7.8		
	Be															
	B		5													
	C															
	N															
	S								1370	680	855			715		
	F													22.4		
	Cl										3.21		4.0			
	Br							0.008				13.7		0.018		
	Cu		18						9	29				10.6		
	Zn							1.05	<1.5	17				3.33		
(ppb)	I											0.69				
	At															
	Ga		5000											3240		
	Ge							2.8						50		
	As													0.5		
	Se							123						126		
	Mo															
	Tc															
	Ru												0.5(a)			
	Rh															
	Pd															
	Ag							1								
	Cd							0.68								
	In							0.6								
	Sn															
	Sb							0.035								
	Te							6.2								
	Cs							42						37		
	Ta			460	770									410		
	W													59		
	Re							0.0015								
	Os												0.19			
	Ir							0.0069								
	Pt															
	Au							0.012						0.44		
	Hg															
	Tl							0.24								
	Bi							0.12								
		(1)	(2)	(3)	(3)	(4)	(5)	(6)	(7)	(7)	(8)	(9)	(10)	(11)	(12)	(12)

References and methods:

(1) Helmke and Haskin (1972), Helmke et al. (1973); INAA
(2) Mason et al. (1972); general silicate analysis, gravimetric, flame photometry, colorimetry, emission spec.
(3) Fruchter et al. (1973); INAA
(4) Tatsumoto et al. (1972); ID/MS
(5) Keith et al. (1972); gamma ray spectrometry
(6) Ganapathy et al. (1973); RNAA
(7) Duncan et al. (1975); XRF
(8) Gibson et al. (1975); combustion
(9) Jovanovic and Reed (1976b); neutron and photron activation, colorimetry
(10) Jovanovic and Reed (1977); INAA
(11) Wanke et al. (1976); XRF, RNAA, INAA
(12) Unruh and Tatsumoto (1977); ID/MS

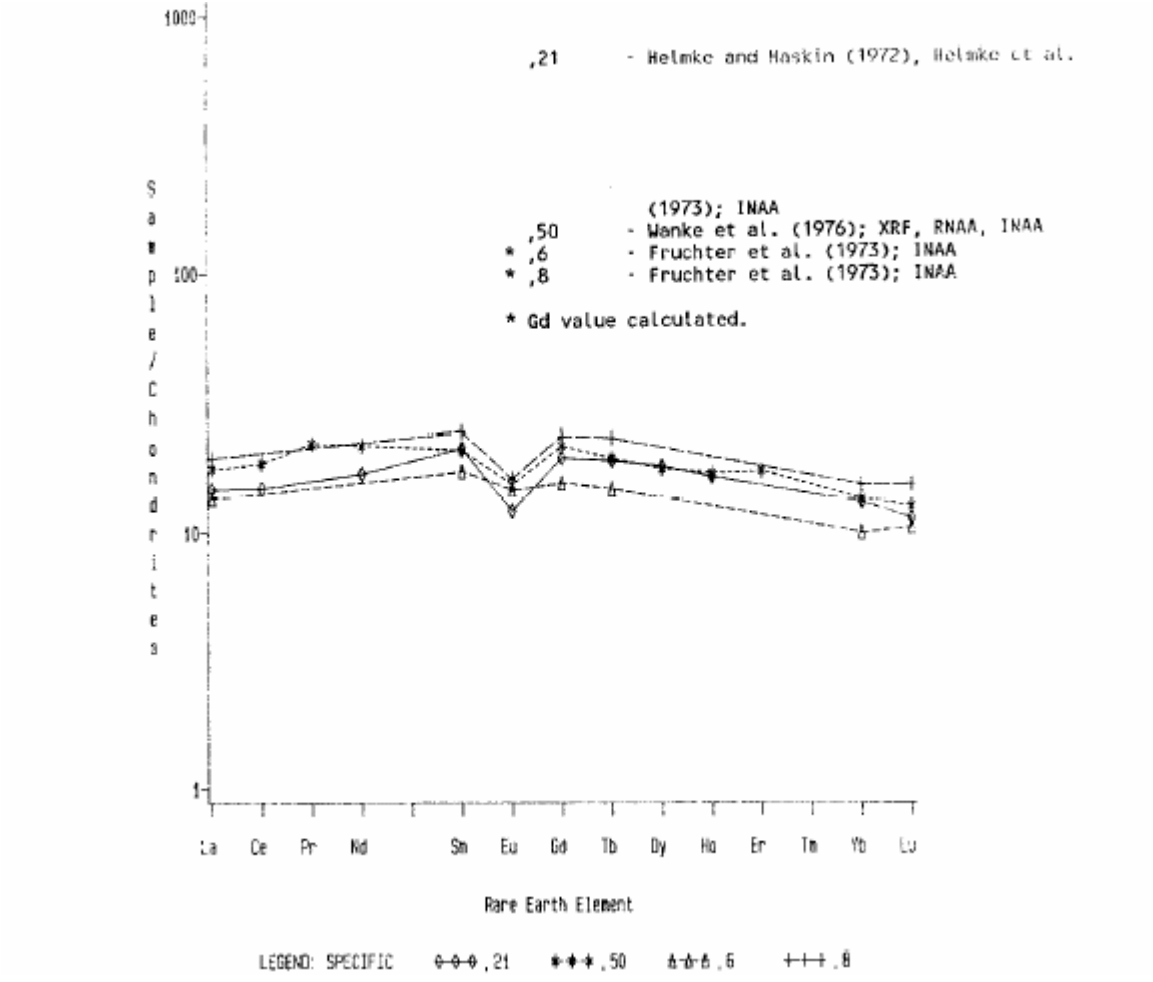

Figure 6. Rare earths in bulk rock samples.

(20 to 50%) of the U, Th, and Pb were easily leachable, with the implication that such portions originally resided on grain, boundaries, in microfractures, or in interstices. There is an apparent depletion of ^{207}Pb relative to ^{206}Pb on the leached fractions (Fig. 8), and an enrichment of ^{208}Pb. The trends cannot be explained by Pb contamination. The actual ages defined by the trends are both older than the actual crystallization age of about 3.4 b.y. and probably neither has any age significance. Similar trends on the U-Pb evolution diagram (Fig. 9) also have no real age significance other than that the lower

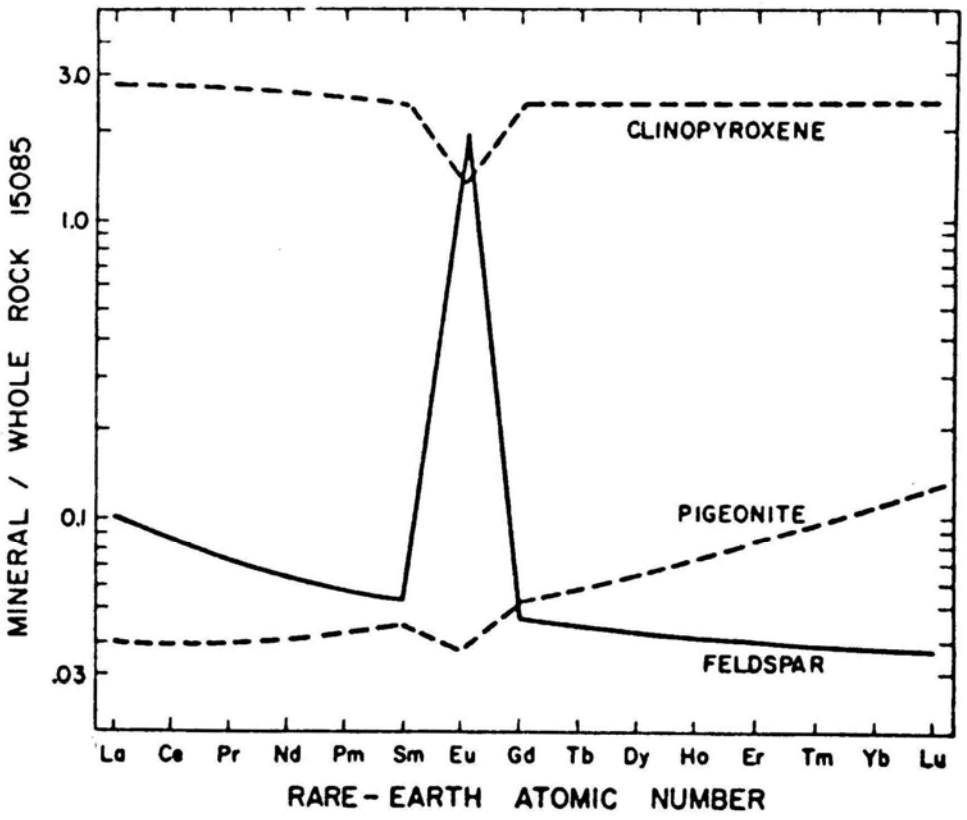

Figure 7. Rare earths in mineral separates
(Helmke et al., 1973)

concordia intercepts indicate some sort of post-crystallization disturbance. Individual parent-daughter diagrams for ^{206}Pb, ^{207}Pb, and ^{208}Pb are shown as Figure 10. The ^{206}Pb diagram shows an "age" for the residues of 3.44 ± 0.22 b.y. The ^{207}Pb shows an opposite effect: the leaches are younger, indicating ^{207}Pb depletion in grain boundaries. The anomalously old ages (3.6 b.y. leaches, 3.79 b.y. residues) suggest enrichment of ^{207}Pb relative to uranium. The ^{208}Pb shows relationships similar to the ^{206}Pb, with a combined "age" of 3.59 ± 0.25 b.y. Preferential leaching alone cannot account for the trends in Figure 10.

The distinct trends of the residues and leaches appear to represent either continuous or episodic post-crystallization disturbances, but a unique interpretation is not possible. Unruh and Tatsumoto (1977) proposed a two-stage, KREEP-mixing model to explain the U-Pb evolution in mare basalts, a model compatible with Rb-Sr and Sm-Nd data, but if the primary differentiation occurred at a time distinctly different from lunar accretion then a more complex model is required. They concluded that (according to reported and calculated U and Pb partition coefficients) the initial $^{238}U/^{207}Pb$ (μ) of the moon was quite high, i.e., 100 to 300.

Rosholt and Tatsumoto (1973) and Rosholt (1974) discussed α-spectrometry measurements of $^{232}Th/^{230}Th$ as compared with the value for that ratio expected from the $^{232}Th/^{238}U$ concentration ratio. The expected/measured ratio is 1.27, and its significance was discussed by Rosholt (1974).

EXPOSURE AND TRACKS: Keith et al. (1972) reported disintegration count data for ^{26}Al, ^{22}Na, ^{54}Mn, ^{56}Co, and ^{46}Sc. The ^{26}Al was saturated, implying a surface residence of a few million years. Yokoyama et al. (1974), correcting for composition, agreed that ^{26}Al was saturated.

Bhandari et al. (1972) and Bhattacharya 9t al. (1975) measured track densities in two surface chips of 15085. Densities of 6 and 12 x 10^6 cm^{-2}, and "suntan" ages of less than 1 m.y. were determined. Bhattacharya et al. (1975) reported the ages as less than 10 to 30 m.y.

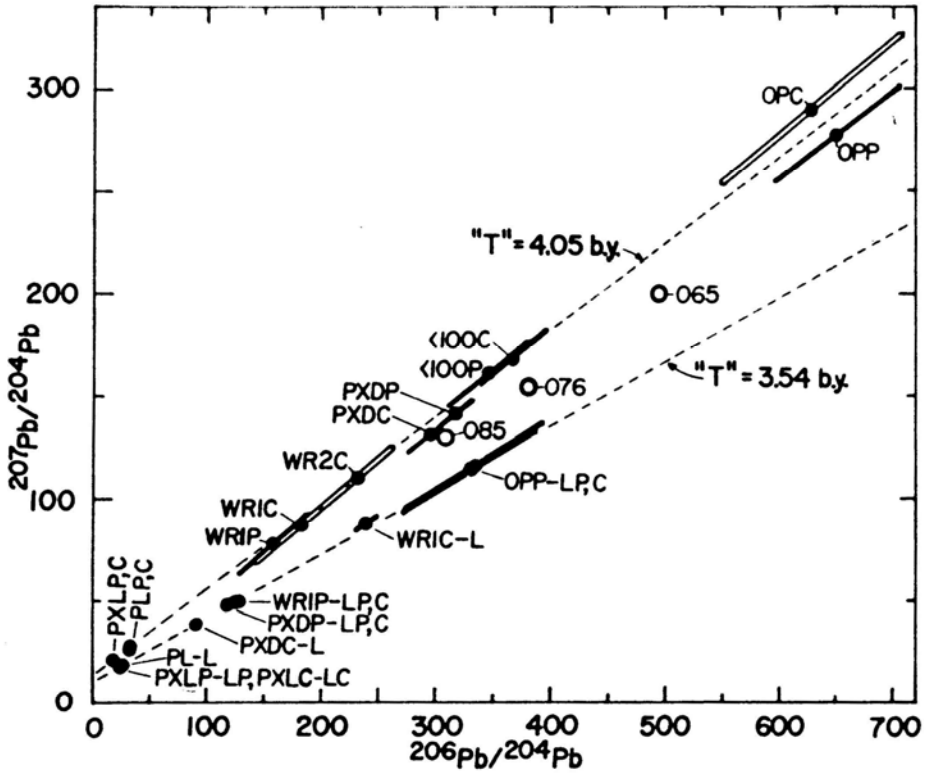

$^{206}Pb/^{204}Pb$ vs. $^{207}Pb/^{204}Pb$ plot of mineral separate residues and leaches from 15085. The leaches and residues define distinctly different trends yielding apparent ages of 3.54 ± 0.06 and 4.05 ± 0.08 b.y., respectively. The ages probably have no significance, and are much older than Rb–Sr and Sm–Nd ages of ~3.3–3.4 b.y. for this rock. The two trends suggest that post-crystallizational disturbances have affected the Pb–Pb system. The "old" ages suggest ^{207}Pb enrichment from an outside source or lack of isotopic homogenization prior to crystallization.

Figure 8. $^{206}Pb/^{204}Pb$ vs. $^{207}Pb/^{204}Pb$ in mineral separate residues and leaches from 15085 (Unruh and Tatsumoto, 1977).

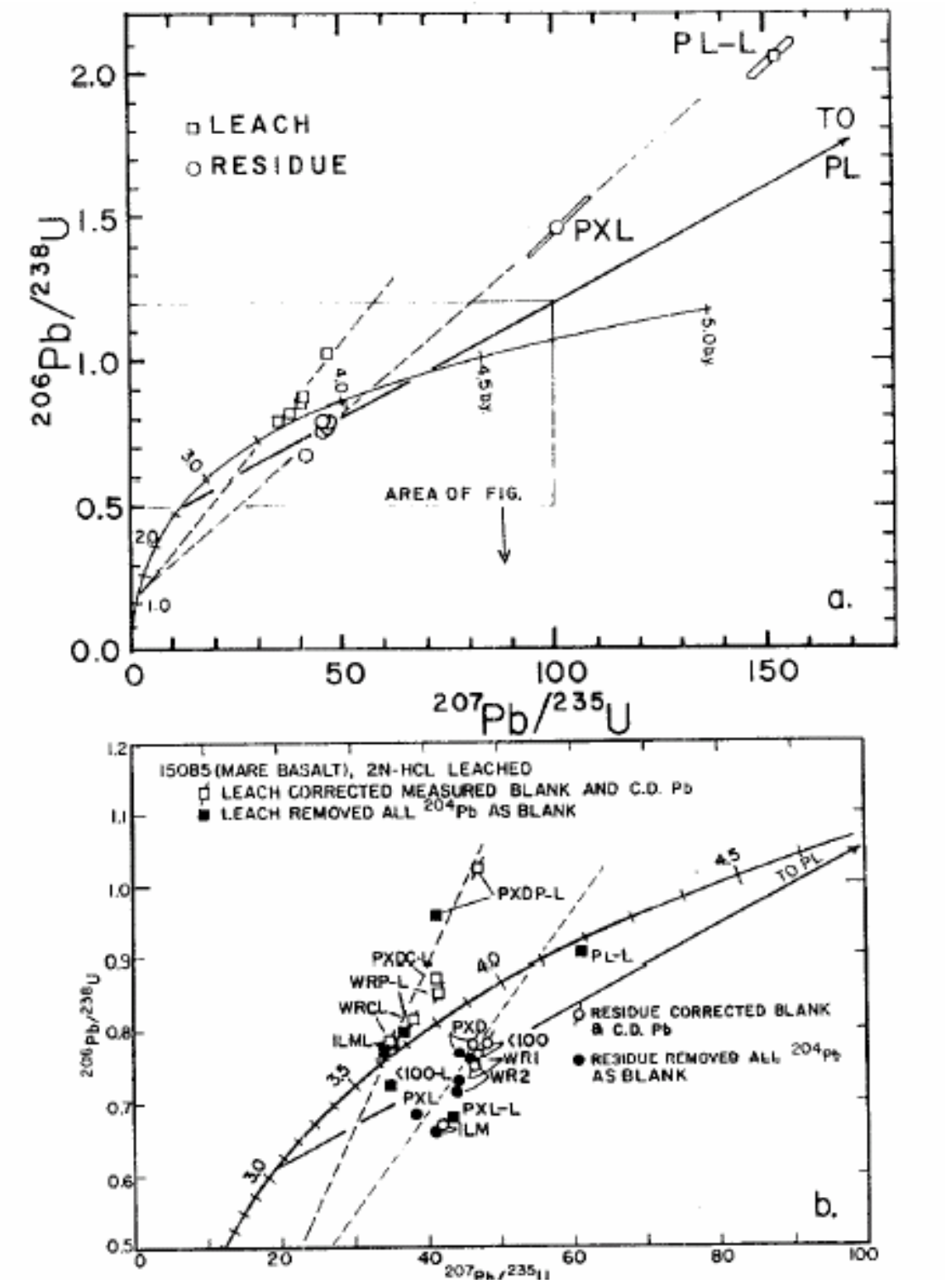

Figure 9. U-Pb evolution diagram. Corrected for Canyon Diablo troilite Pb (open symbols) and all ^{204}Pb as modern terrestrial (blank; closed symbols).

Leach = squares. Residue = circles. (Unruh and Tatsumoto, 1977).

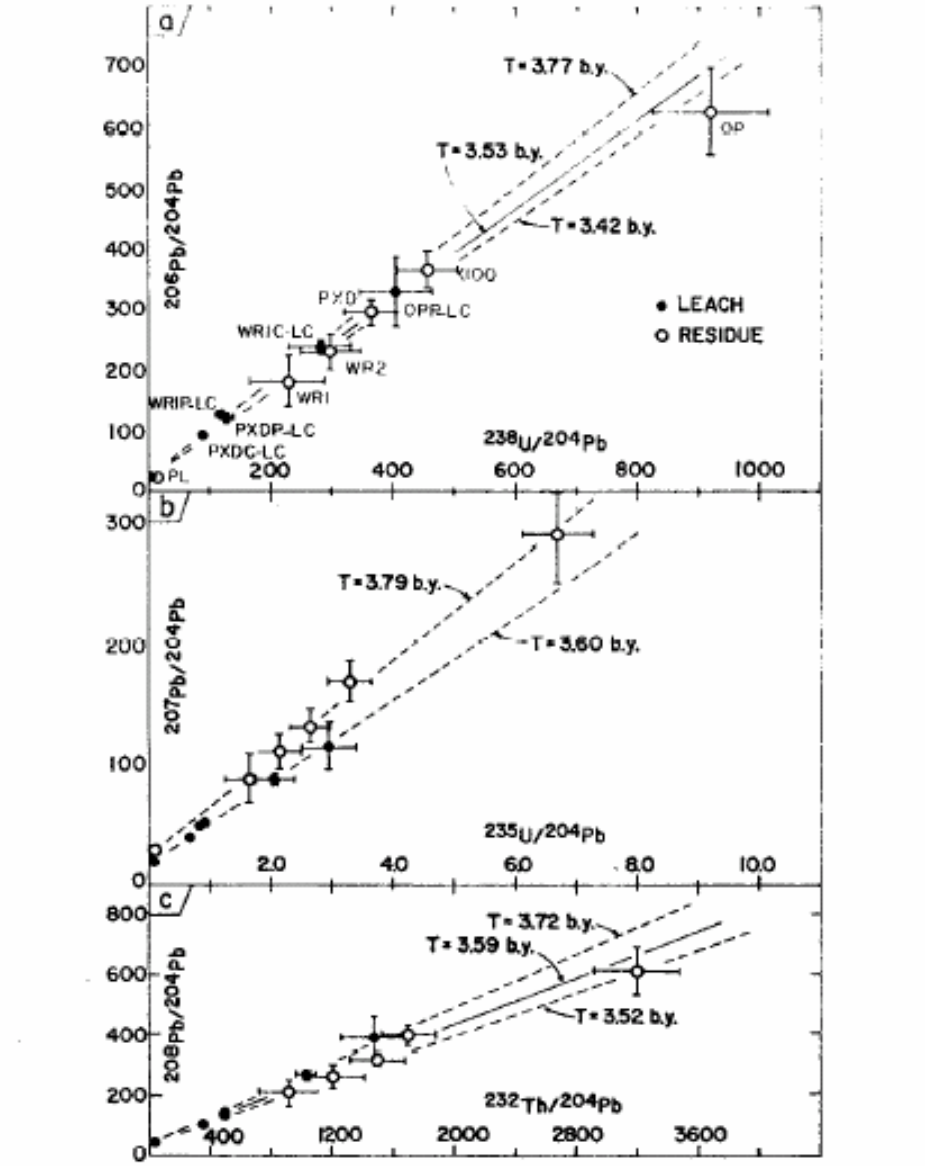

U–Pb and Th–Pb parent-daughter evolution diagrams for 15085. (a) $^{238}U/^{204}Pb$ vs. $^{206}Pb/^{204}Pb$ plot. The residues (open circles) define an "age" (lower broken line) of 3.42 ± 0.22 b.y. (95% confidence) which is in agreement with Rb–Sr and Sm–Nd ages. The leaches (closed circles) define a 3.77 ± 0.26 b.y. "age" (upper broken line). Combination of the data (solid line) yields a 3.53 ± 0.09 b.y. "age". (b) $^{235}U/^{204}Pb$ vs. $^{207}Pb/^{204}Pb$ plot. The residues (solid) line define a 3.79 ± 0.10 b.y. apparent age. The leach data (broken line) yield a 3.60 ± 0.12 b.y. "age". Both ages are older than the Rb–Sr and Sm–Nd ages which suggests ^{207}Pb enrichment relative to U (addition of "old" Pb). (c) $^{232}Th/^{204}Pb$ vs. $^{208}Pb/^{204}Pb$ plot. The residue trend (lower broken line) defines a 3.5 ± 0.5 b.y. apparent age, whereas the leaches (upper broken line) define a 3.72 ± 0.12 b.y. "age". However this very old age is mostly controlled by OP–L, which appears to have suffered Th–Pb fractionation during leaching. The combined data (solid line) yield an apparent age of 3.59 ± 0.25 b.y.

Figure 10. U-Pb and Th-Pb parent-daughter evolution diagrams. Residues = open circles. Leaches = closed circles.

(Unruh and Tatsumoto, 1977).

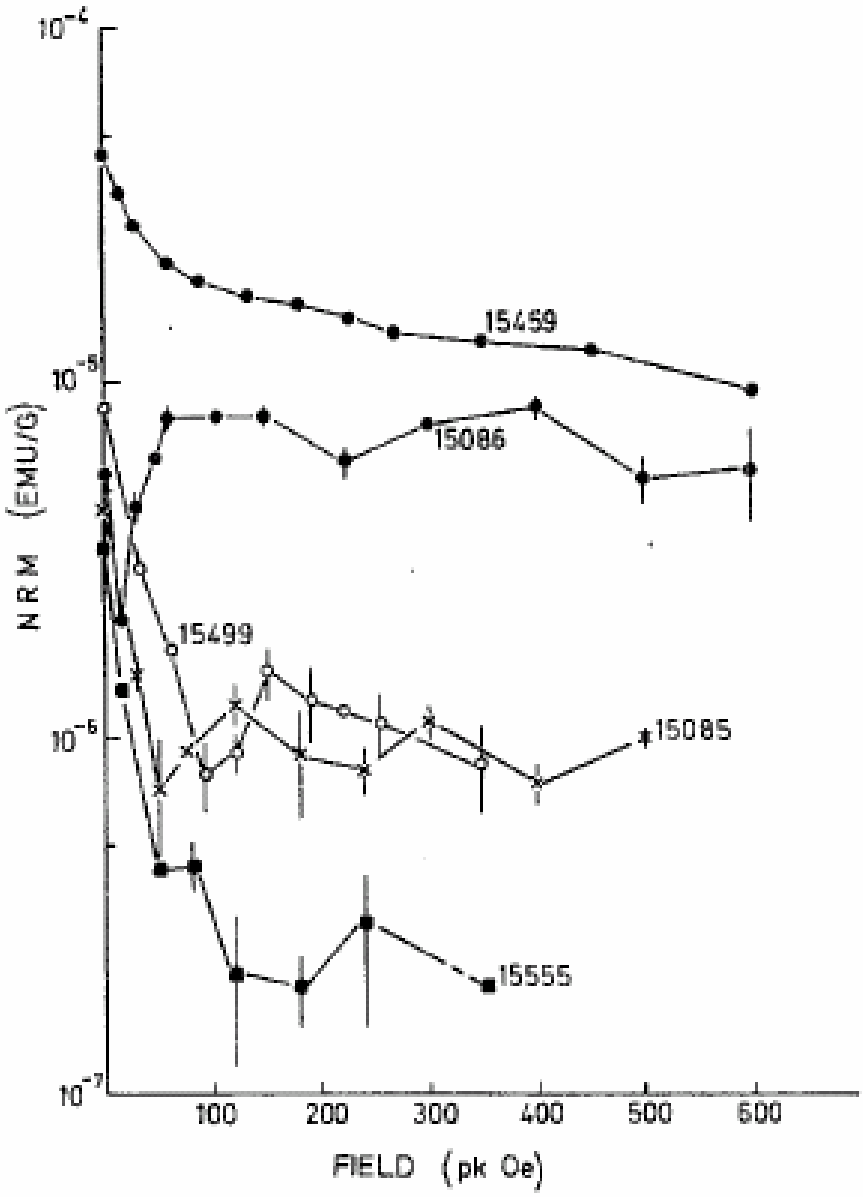

Figure 11. Alternating field demagnetization of 15085 and some other Apollo 15 samples. 15459 and 15086 (higher NRM) are breccias; the other samples are mare basalts (Collinson et al., 1973).

PHYSICAL PROPERTIES: Collinson et al. (1972, 1973) determined the magnetic characteristics of two whole-rock samples. They had as-received natural remanent magnetisms (NRM) of 8.7, and 7.1, x $l0^{-6}$ emu/g (Fig. 11). ,31 showed an approximately constant direction of NRM after removal of the soft components (AF demagnetization). Thermal demagnetization up to 500°C for ,32 produced the same general behaviour in

NRM as AF treatment, but at high temperatures the directions scattered. Iron is the carrier of the magnetization. There is some evidence for anomalous variation in intensity during AF demagnetization. In rock magnetism studies, the two samples produced almost identical induced magnetization curves. They failed to saturate in a field of 8 KOe, and the slope of the graph at this field is 31 x 10^{-6} emu g^{-1} Oe^{-1}, which is still a significant fraction of the induced susceptibility. In thermoremanent magnetic studies, a sudden decrease in magnetization occurred at -150°C when being warmed from -196°C to 20°C. Measurements on a crystal near ulvospinel in composition gave almost identical results.

Greenmann and Gross (1972) reported luminescence studies of 15085, tabulating and diagramming peak wavelength, bandwidths, and band efficiencies for soft x-ray irradiation.

PROCESSING AND SUBDIVISIONS: A large chip (,2) was first removed from the "B"/"E" end corner, and split to produce daughters ,3 to ,9. ,4 was potted and produced thin sections ,11 to ,19 and ,23 to ,26. Several allocations were made from the other chips. Further chipping (Fig. 12) produced ,29 to ,33 from different parts of the sample, with ,33 producing thin section ,77; ,78; and ,16; some thin section mix-ups with sample 15285 were made and corrected. In 1974, large chips were made to produce samples for remote storage (,43, 20.00 g; ,44, 8.21 g; ,45, 27.99 g) at Brooks, producing several other daughters of small chips (,40 to ,56). In 1982, chipping was done to obtain about 10 g of representative sample, which was crushed to a medium sand size (,143). 2.3 g were allocated for chemical analysis (,152), the rest is stored. This action also produced a large piece (,142, 53.0 g) and other chips and fines.

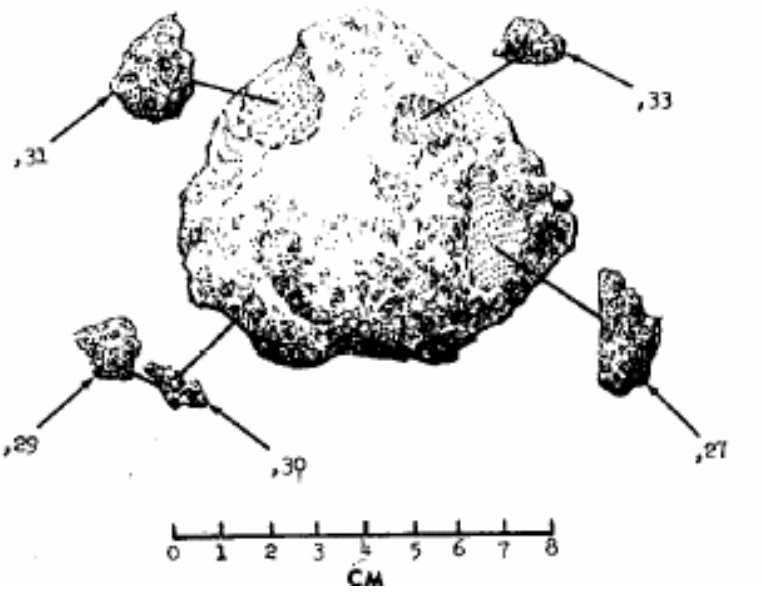

Figure 12. Part of the chipping of 15085.